

Tuning Synthesis Parameters for Eco-friendly Iron Oxide Nanoparticles Using *Pimenta dioica* Extract

Bolaj AR*, Mahaparale SP

Department of Pharmaceutical Chemistry, Dr. D. Y. Patil College of Pharmacy, Akurdi, Pune 411044, India.

Received: 13rd Aug, 2024; Revised: 29th Oct, 2024; Accepted: 17th Nov, 2024; Available Online: 25th Dec, 2024

ABSTRACT

The fabrication of iron oxide nanoparticles (IONPs) through green synthesis techniques with *Pimenta dioica* extract, focusing on the effects of extract proportion, reaction time, temperature, pH, and stirring speed (RPM) on nanoparticle properties. The aim is to identify optimal conditions for producing IONPs with desirable characteristics for biomedical applications. The process involved combining extract, FeCl₂ (Ferric chloride) and FeSO₄ (ferrous sulphate) with 25% ammonia, then subjecting to calcination. The properties of the obtained nanoparticles were assessed, including particle size, zeta potential, thermal stability, magnetization, entrapment efficiency, and drug release. Optimal conditions were found to be a 2:1 extract proportion, 2-3 hours synthesis time, 60-80°C temperature, pH of 10-11, and 900 RPM. Under these conditions, the IONPs exhibited small particle sizes, high thermal stability, high magnetization, and high drug release rates. This study highlights the potential of *Pimenta dioica* extract in the green synthesis of IONPs, providing insights for optimizing nanoparticle synthesis for medical applications.

Keywords: IONPs, *Pimenta dioica* Extract, Reaction Parameters, Nanoparticle Characterization, Magnetization.

How to cite this article: Bolaj AR, Mahaparale SP. Tuning Synthesis Parameters for Eco-friendly Iron Oxide Nanoparticles Using *Pimenta dioica* Extract. International Journal of Drug Delivery Technology. 2024;14(4):2323-30 doi: 10.25258/ijddt.14.4.53

Source of support: Nil.

Conflict of interest: None

INTRODUCTION

Iron oxide nanoparticles (IONPs) have a wide range of applications in biomedical fields, as their magnetic characteristics and biocompatibility, IONPs are crucial for drug delivery, enabling targeted transport and controlled release. They also enhance Magnetic Resonance Imaging (MRI) contrast, support cancer hyperthermia treatment, and advance biosensing technologies. This research investigates the synthesis, characterization, and optimization of IONPs, highlighting their potential to revolutionize medical treatments and biotechnological advancements. It discusses their role in targeted drug delivery, imaging, and therapeutics due to their magnetic properties. The study also highlights advancements in biotechnology facilitated by these nanoparticles, emphasizing their potential in improving diagnostic techniques and therapeutic outcomes in various medical applications.¹ Iron-based nanomaterials have attracted significant interest due to their distinctive properties, including high reactivity, magnetic behavior, and the ability to be easily functionalized, which makes them versatile for numerous applications across various fields. To sustainably leverage the advantages of nanotechnology, it is crucial to adopt green synthesis approaches, reducing potential environmental harm. Green synthesis refers to the production of nanomaterials using environmentally benign methods, often leveraging biological entities like plants, bacteria, and fungi, or employing eco-friendly chemicals. Plant extracts are attractive for nanoparticle synthesis because they are rich in natural compounds like phenolics and flavonoids, which can reduce metal ions and stabilize the nanoparticles. This

method is eco-friendly, avoiding harmful chemicals, and it also improves the compatibility of the nanoparticles with biological systems, making them more suitable for medical applications like drug delivery and cancer therapy. The leaves are particularly rich in antioxidants, flavonoids, and other bioactive compounds, which significantly boost their efficiency in green synthesis. These methods not only reduce the environmental impact of nanomaterial production but also enhance the biocompatibility and functional characteristics of the final products.^{2,3} Green synthesis of nanoparticles provides numerous benefits compared to conventional chemical methods. It is eco-friendly, minimizing the use of harmful solvents and chemicals by leveraging natural resources like plant extracts. This method is also cost-efficient due to the abundance and low expense of these natural materials and the straightforward processes involved. Furthermore, green synthesized nanoparticles tend to be more biocompatible and safer for biomedical applications, including drug delivery and cancer treatment. The procedures typically operate under mild conditions, reducing energy consumption and further cutting costs.⁴ Various factors impact the green synthesis of nanoparticles, influencing their size, shape, and stability. The choice of biological source (such as plant extracts, bacteria, or fungi) determines the bioactive compounds available for the reduction and stabilization processes. The concentration of these extracts and the pH of the reaction medium are crucial, with higher extract concentrations and optimal pH conditions generally leading to smaller and more well-defined nanoparticles. Additionally, temperature and reaction time impact

*Author for Correspondence: patilamruta093@gmail.com

synthesis, with elevated temperatures and shorter reaction times often resulting in smaller particles. Uniform agitation is necessary to ensure even distribution of reactants, and the concentration of metal ions in presence of capping agents, prevent aggregation, also play significant roles. By carefully managing these factors, researchers can tailor nanoparticles to meet specific requirements for various purposes.⁵

In this research, we used extract of *Pimenta dioica*. *Pimenta dioica* (Linn.) Merrill, commonly known as allspice, is prized for its rich array of chemical constituents that contribute to its aromatic allure and diverse applications. Chief among these compounds is eugenol, which imparts a clove-like aroma, accompanied by cineole, methyl eugenol, and myrcene. These components not only define its spicy fragrance but also underpin its multifaceted uses. Culinary traditions worldwide embrace allspice for its ability to enhance dishes with a unique blend of flavors reminiscent of cloves, cinnamon, and nutmeg, making it a staple in Caribbean, Latin American, and Middle Eastern cuisines. Beyond the kitchen, allspice is revered for its medicinal properties, offering antioxidant, anti-inflammatory, and antimicrobial benefits. It has historically been utilized to alleviate digestive ailments, muscle discomfort, and dental issues. In addition to its culinary and medicinal roles, allspice finds application in perfumery and

cosmetics, where its warm, aromatic profile enriches fragrances, soaps, and skincare products. Furthermore, its natural antimicrobial qualities have rendered it useful as a preservative in food preservation methods and traditional embalming practices. Altogether, *Pimenta dioica* stands as a versatile spice celebrated for its flavor, fragrance, and therapeutic potential across various cultural and industrial domains.⁶ In this investigation into IONPs synthesis using *Pimenta dioica*, aim to investigate various process parameters including extract proportion, reaction time, pH, RPM, and temperature, and evaluate their respective effects. This research will provide valuable insights for determining optimal parameters when using design software. This approach can help optimize nanoparticle synthesis for desired properties and applications.

MATERIAL AND METHOD

In this study, iron oxide nanoparticles (IONPs) were synthesized using an ethanolic extract from dried *Pimenta dioica* leaves. Ethanol for the extraction was sourced from AnaLab Fine Chemicals, Mumbai. The synthesis used 0.1M Ferric chloride hexahydrate and 0.1M Ferrous sulphate, both from Research Lab Fine Chem Industries, along with 25% ammonia solution from Pallav Chemicals & Solvents Pvt. Ltd., as per prior studies. The Analytical reagent (AR) grade chemicals were used as supplied, without any

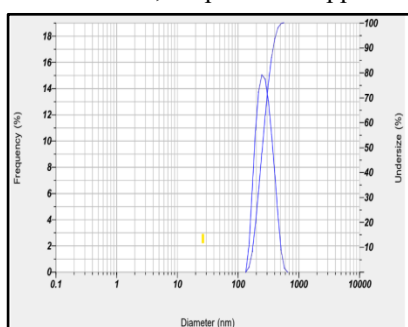


Figure 1: Particle Size of AE2

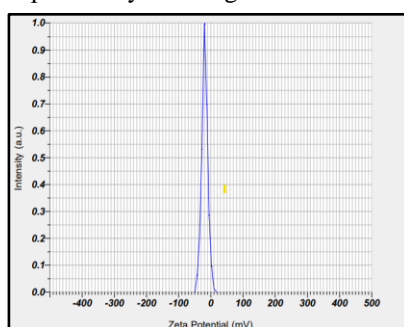


Figure 2: Zeta Potential of AE2

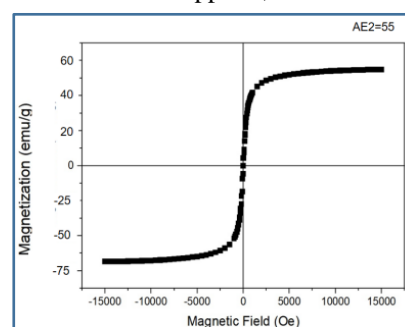


Figure 3: VSM of AE2

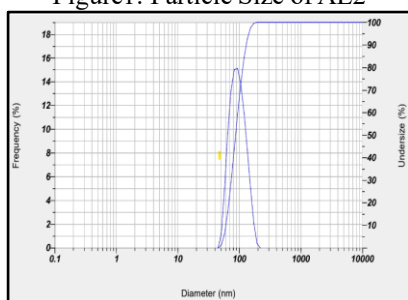


Figure 4: Particle Size of TA2

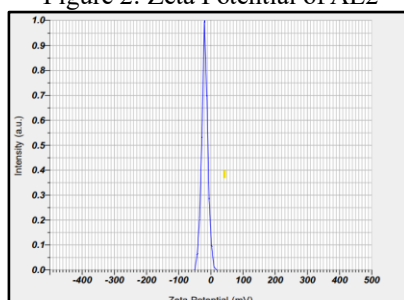


Figure 5: Zeta Potential of TA2

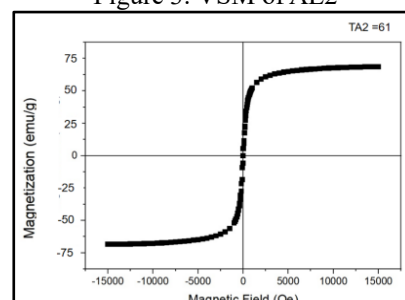


Figure 6: VSM of TA2

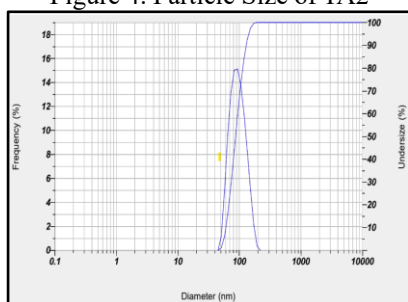


Figure 7: Particle Size of TEA4

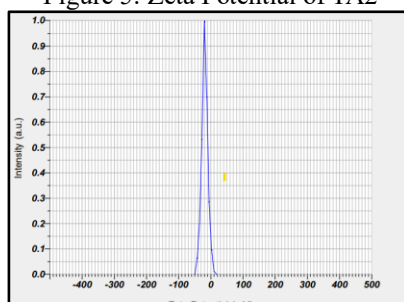


Figure 8: Zeta Potential of TEA4

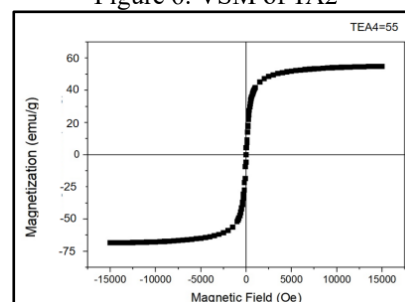


Figure 9: VSM of TEA4

additional purification. For all processes and dilutions, distilled water was employed. Magnetic stirrer (LMMS-300, Labman Scientific Instruments Pvt. Ltd., Chennai) was employed to mix the reaction components, providing control over temperature, Revolution Per Minute (RPM), and time. After synthesis, a centrifuge was used to separate the nanoparticles, and a muffle furnace was used for calcination. These materials and equipment were crucial in ensuring the consistency and reproducibility of the green synthesis method.

Methods

Extraction of *Pimenta dioica* using ethanol

Fresh *Pimenta dioica* leaves were washed, air-dried, and ground into powder. The powder was macerated in 70% ethanol for 72 hours with occasional stirring, then filtered to separate the liquid extract from the marc. The marc was re-macerated until saturation, and the final extract was stored in a dark bottle at 4°C.^{8,9}

IONPs synthesis

An extract of *Pimenta dioica* with 0.1M FeCl₂ and 0.1M FeSO₄ solutions were used for synthesis of IONPs by coprecipitation method, using a 25% ammonia solution, to examine how different process factors affected the characteristics of the final product. Magnetic stirrer was used for mixing the reaction components. Later on, it was centrifuged and calcinated. Following calcination, the precipitate was purified using distilled water and ethanol, and then dried. The dried particles were subsequently evaluated.^{7,10}

Impact of different parameters on synthesis of IONPs

Impact of extract proportion

Different batches were prepared by varying the amount of *Pimenta dioica* extract added to the iron precursors. The ratios of the extract to the 0.1M FeCl₂ and 0.1M FeSO₄ mixture were adjusted to 1:1, 2:1, 3:1, 1:2, and 1:3, with the batches designated as AE1, AE2, AE3, AE4, and AE5, respectively. These experiments were conducted under constant temperature, stirring speed, and duration to

investigate how the proportion of extract affects the synthesis of iron oxide nanoparticles (IONPs).¹¹

Impact of duration

To investigate the impact of reaction duration, different batches were synthesized with varying stirring times. Batch TA1 was stirred over 1 hour, batch TA2 over 2 hours, and batch TA3 over 3 hours.^{12,13}

Impact of temperature

The synthesis process was conducted at the following temperatures: 40°C (TEA1), 50°C (TEA2), 60°C (TEA3), 70°C (TEA4), and 80°C (TEA5), with each batch stirred for one hour.¹³

Impact of pH

pH of the reaction mixture was adjusted to various levels to study its impact on the synthesis of IONPs. pH levels were set to 8, 9, 10, and 11 for batches PA1, PA2, PA3, and PA4, respectively. These mixtures were subsequently stirred under the same conditions.¹⁴

Impact of revolutions per minute (RPM)

The effect of stirring speed on the properties of the synthesized nanoparticles was examined by adjusting the revolutions per minute (RPM). The ethanolic extract was mixed FeCl₂ and FeSO₄ and stirred for a set duration at varying speeds. The stirring rates were 150 RPM (RA1), 300 RPM (RA2), 450 RPM (RA3), 600 RPM (RA4), 750 RPM (RA5), and 900 RPM (RA6), with each batch corresponding to one of these speeds.¹⁵

Evaluation of IONPs

Size distribution and stability

The nanoparticles' size distribution and surface charge were evaluated using dynamic light scattering (DLS) with a Malvern Zetasizer Nano ZS (Malvern Instruments, UK). This technique provides data on particle size, revealing the nanoparticles' uniformity and likelihood of aggregation. Additionally, it measures zeta potential, which indicates surface charge and is crucial for assessing nanoparticle stability in biological systems.^{16,17}

Thermogravimetric analysis (TGA)

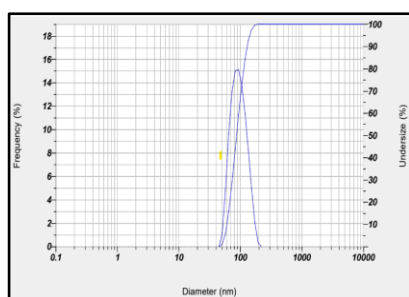


Figure 10: Particle Size of PA4

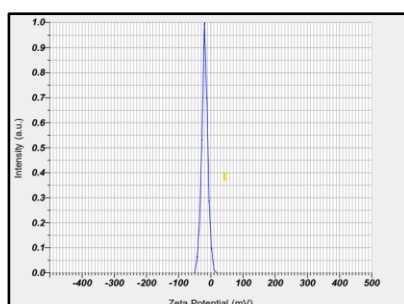


Figure 11: Zeta Potential of PA4

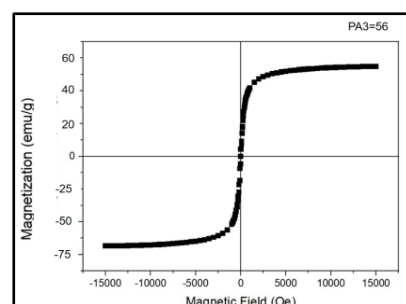


Figure 12: VSM of PA4

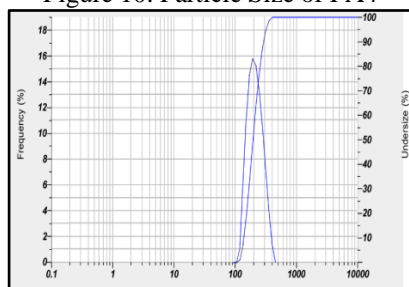


Figure 13: Particle Size of RA6

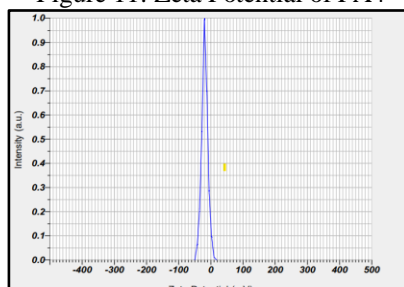


Figure 14: Zeta Potential of RA6

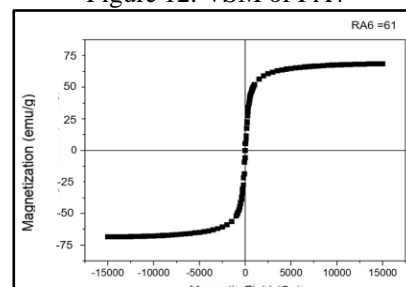


Figure 15: VSM of RA6

Using a TGA Q500 (TA Instruments, USA), the thermal stability of the nanoparticles was tested. The sample was heated in a nitrogen atmosphere, starting from room temperature and increasing to 800°C at a rate of 10°C per minute, while monitoring weight loss as the temperature rose.¹⁸

Vibrating sample magnetometer (VSM)

A vibrating sample magnetometer (VSM), specifically the Microsense EZ, was used to examine the magnetic properties of the nanoparticles. An external magnetic field was applied to the samples to determine their coercivity, retentivity, and saturation magnetization.¹⁶

Entrapment efficiency (EE)

A 10 mg sample of nanoparticles (NPs) was dispersed in 10 mL of methanol and stirred for 1 hour. The supernatant was then separated, and the eugenol (EU) content was quantified using UV-visible spectroscopy (Shimadzu) at 282 nm to

evaluate the eugenol entrapment efficiency in the NPs. The entrapment efficiency (%EE) was determined using the following formula^{19,20}:

$$EE (\%) = \frac{\text{Total amount of loaded eugenol}}{\text{initial amount of eugenol}} \times 100$$

Drug release studies

To evaluate the drug release from the nanoparticles, 5 mg of the nanoparticles were dispersed in 2 mL of phosphate-buffered saline (PBS) containing 2% (v/v) Tween 80 and placed in a dialysis bag with a 12 kDa molecular weight cutoff (MWC0). The dialysis bag was immersed in 25 mL of PBS, and at designated time intervals, 2 mL of the dialysate was collected and replaced with fresh PBS. The concentration of eugenol in the dialysate was quantified using UV-visible spectroscopy at 282 nm.^{19,20}

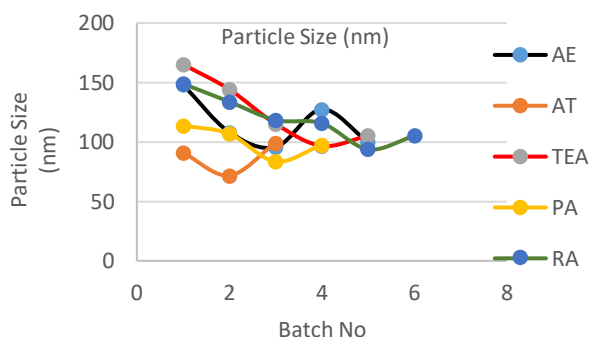


Figure 16: Reaction Parameters & Particle Size

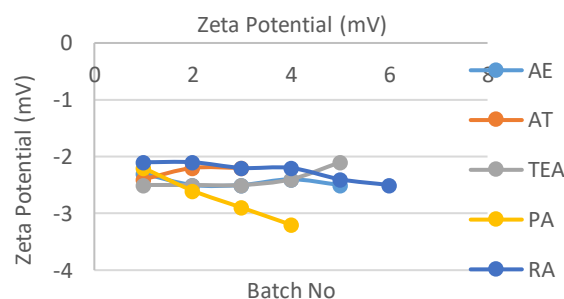


Figure 17: Reaction Parameters & Zeta Potential

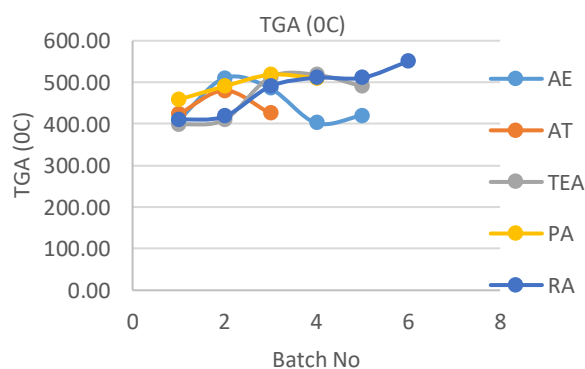


Figure 18: Reaction Parameters & TGA

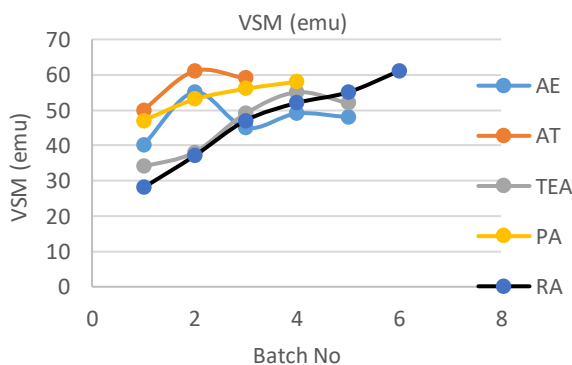


Figure 19: Reaction Parameters & VSM

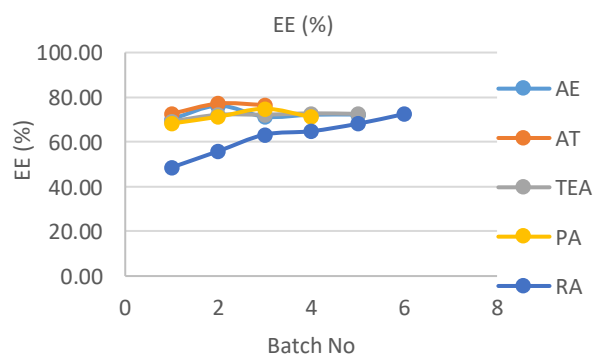


Figure 20: Reaction Parameters & EE

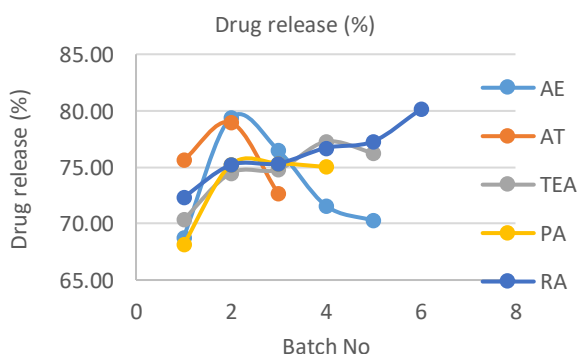


Figure 21: Reaction Parameters & Drug release

RESULTS

Impact of extract proportion

The nanoparticle batches were compared based on several key properties. Particle size varied from the smallest in AE3 at 95.7 nm to the largest in AE1 at 148.1 nm, with AE2 and AE5 having intermediate sizes of 98.2 nm and 99.8 nm, respectively. The zeta potential ranged from -2.3 mV for AE1, which was the least negative, to -2.5 mV for AE2, AE3, and AE5, indicating slightly more negative surface charges in these batches compared to AE1. Thermal stability was highest for AE2, which withstood up to 510.25°C before significant weight loss, suggesting superior thermal resistance. In contrast, AE4 had the lowest thermal stability at 402.11°C. Regarding magnetic properties, AE2 demonstrated the highest magnetization at 55 emu/g, whereas AE1 had the lowest at 40 emu/g. Batches AE3, AE5, and AE4 had magnetization of 45, 49, and 48 emu/g, respectively. Entrapment efficiency (EE) was highest for AE2 at 76.23%, indicating the best drug loading capability. AE1 had the lowest EE at 70.20%, while AE3, AE4, and AE5 had efficiencies of 71.28%, 72.18%, and 72.26%, respectively. For drug release, AE2 showed the highest release rate at 79.38%, whereas AE1 had the lowest at 68.77%. AE3, AE4, and AE5 had intermediate release rates, with AE3 at 76.49%, AE4 at 71.60%, and AE5 at 70.26%. Based on these characteristics, AE2 emerges as the optimized batch due to its highest drug release rate and superior thermal stability, higher entrapment efficiency and its particle size, zeta potential and magnetic properties are shown in Figure 1, Figure 2, Figure 3 respectively.

Impact of duration

The performance of the nanoparticle batches was assessed across several parameters. Particle size varied, with TA2 being the smallest at 71.8 nm and TA3 the largest at 99.2 nm. TA1 had an intermediate particle size of 90.9 nm. Zeta potential measurements were closest for TA2 and TA3, both at -2.2 mV, suggesting slightly better stability than TA1, which had a zeta potential of -2.4 mV. In terms of thermal stability, TA2 demonstrated the highest resistance, enduring temperatures up to 480.26°C before significant weight loss. This contrasts with TA1 and TA3, which had lower thermal stabilities of 423.12°C and 425.26°C, respectively. For magnetic properties, TA2 led with a magnetization of 61 emu/g, surpassing TA3 and TA1, which had magnetization of 59 emu/g and 50 emu/g, respectively. Entrapment efficiency (EE) was highest in TA2 at 77.17%, indicating the most effective drug loading. In comparison, TA3 and TA1 had efficiencies of 76.52% and 72.62%, respectively. Regarding drug release, TA2 at highest rate 78.95%, TA1 at 75.6% while TA3 at 72.65%. Overall, TA2 is highlighted as the optimized batch due to its superior drug release rate, highest entrapment efficiency, and best thermal stability. Although it slightly outperforms TA3 in key performance metrics, the differences between the two batches are minimal, making both promising candidates for future applications. Maintaining the strengths of TA2 in particle size, zeta and magnetic properties, shown in Figure 4, Figure 5 and Figure 6.

Impact of temperature

The nanoparticle batches were evaluated on various parameters, revealing distinct performance characteristics. Particle size varied significantly, with TEA1 having the largest size at 165.2 nm and TEA4 the smallest at 96.7 nm. TEA2 and TEA5 had sizes of 144.2 nm and 105.2 nm, respectively, while TEA3 measured 115.2 nm. Zeta potential values were fairly uniform across the batches, with TEA1, TEA2, TEA3, and TEA4 all at -2.5 mV, indicating consistent surface charge properties. TEA5 had a slightly less negative zeta potential of -2.1 mV. Regarding thermal stability, TEA4 showed the highest resistance, maintaining stability up to 518.16°C before significant weight loss occurred. This is higher than TEA1, which had the lowest stability at 398.26°C, and TEA2, TEA3, and TEA5, with stabilities of 410.20°C, 512.26°C, and 490.26°C, respectively. For magnetic properties, TEA4 achieved the highest magnetization at 55 emu/g, exceeding the magnetization of TEA5 at 52 emu/g, TEA3 at 49 emu/g, TEA2 at 38 emu/g, and TEA1 at 34 emu/g. Entrapment efficiency (EE) was also highest for TEA4 at 72.80%, demonstrating the most effective drug loading. TEA3 and TEA5 had efficiencies of 72.20% and 72.56%, respectively, while TEA1 and TEA2 had slightly lower efficiencies at 69.21% and 72.15%. In terms of drug release, TEA4 led with the highest rate of 77.25%, followed by TEA5 at 76.25%, TEA3 at 74.79%, TEA2 at 74.47%, and TEA1 at 70.33%. TEA4 was identified as the optimized batch due to its superior performance in critical areas such as thermal stability, drug release rate, and magnetic properties, representing the most balanced and effective combination of attributes. Future research should aim to maintain these strengths in TEA4 while investigating potential improvements in particle size and other characteristics. TEA3 and TEA5 also showed comparable results, indicating that more specific studies are needed to further refine and differentiate the batches. Its present results were shown in Figure 7, Figure 8 and Figure 9.

Impact of pH

The evaluation of the nanoparticle batches showed notable differences in their characteristics. Particle size ranged from PA3, the smallest at 83.5 nm, to PA1, the largest at 113.8 nm. PA2 and PA4 had intermediate sizes of 106.8 nm and 97.5 nm, respectively. Zeta potential values varied, with PA1 having the least negative value at -2.2 mV, and PA4 having the most negative at -3.2 mV. PA2 had zeta potentials of -2.6 mV and PA3 is of -2.9 mV, indicating PA4 has most negative surface charge among the batches. In terms of thermal stability, PA3 exhibited the highest stability, withstanding temperatures up to 518.26°C before significant weight loss occurred. This is superior to PA1 at 458.20°C, PA2 at 490.26°C, and PA4 at 510.23°C. Regarding magnetic properties, PA4 demonstrated the highest magnetization at 58 emu/g, outperforming PA3 at 56 emu/g, PA2 at 53 emu/g, and PA1 at 47 emu/g. For entrapment efficiency (EE), PA3 had the highest value at 74.85%, indicating the most effective drug loading. PA2 and PA4 had efficiencies of 71.25% and 71.20%, respectively, while PA1 had the lowest at 68.26%. Drug release rates were comparable across batches, with PA3 leading at 75.33%, followed closely by PA4 at 75.02%.

PA2 at 75.21%, and PA1 at 68.12%. Overall, PA3 stands out as the optimized batch due to its superior thermal stability, highest entrapment efficiency, and effective drug release rate. It offers the best combination of key performance metrics, making it the most suitable candidate for further research and development. PA4 demonstrated results close to PA3, indicating that further differentiation and analysis are required to refine their differences. The present study of PA3's properties like particle size and other characteristics shown in Figure 10, Figure 11 and Figure 12.

Impact of revolutions per minute (RPM)

The particle sizes ranged from 148.9 nm (RA1) to 93.8 nm (RA5), with zeta potential values between -2.1 mV (RA1, RA2) and -2.5 mV (RA6). Thermal stability, as indicated by TGA values, increased from 410.25 (RA1) to 550.26 (RA6). Magnetization values, measured by VSM, ranged from 28 (RA1) to 61 (RA6). Encapsulation efficiency (EE) improved from 48.59% (RA1) to 72.48% (RA6), and drug release rates increased from 72.32% (RA1) to 80.12% (RA6).

The optimized batch, RA6 with 105.1 nm particle size (Figure 13), -2.5 mV zeta potential (Figure 14), a TGA 550.26, a VSM value of 61emu (Figure 15), an EE of 72.48%, and a drug release rate of 80.12%, demonstrating superior performance across all evaluated metrics compared to the other batches.

DISCUSSION

By using *Pimenta dioica* extract, the formed iron oxide nanoparticles (IONPs) evaluated against various process parameters, including extract proportion, reaction time, temperature, pH, and RPM. The aim was to determine the optimal conditions for producing IONPs with desirable properties for medical applications drug delivery and imaging etc. The proportion of *Pimenta dioica* extract significantly influenced the properties of the synthesized IONPs. The optimal batch (AE2) exhibited the smallest particle size, highest thermal stability, and highest magnetization. This batch also had the highest drug release rate, making it suitable for drug application. Variations in particle size and stability across different extract proportions highlight the importance of the extract's phytochemical content in nanoparticle synthesis. Synthesis time made impact on characteristics of IONPs. A synthesis time of 2 to 3 hours is ideal for producing IONPs with optimal properties. The results suggest that shorter synthesis times may not provide sufficient reduction and stabilization of iron ions, while extended durations could promote aggregation and larger particle sizes. However, more precise optimization within this time range is required to fine-tune the balance between particle size and stability. Temperature variations significantly affected the properties of the IONPs. Synthesis temperature in the range of 60°C to 80°C is ideal for producing IONPs with optimal properties. Within this range, higher temperatures likely enhance the reduction rate of iron ions, improve crystallinity, and boost magnetic properties. Further refinement in this temperature window could help optimize particle size and performance. The pH of the synthesis had a substantial impact on the properties of the IONPs. The

optimal batch (PA3) exhibited the smallest particle size, highest thermal stability, highest magnetization, and highest drug release rate, suggesting that a pH of 10 is ideal for producing IONPs with optimal properties. However, batches synthesized at pH 10 to 11 also showed promising results, indicating that further optimization within this pH range could enhance the nanoparticles' performance. The results indicate that the pH influencing the ability to reduce and stabilize the iron ions. The stirring speed (RPM) during synthesis significantly influenced the properties of the IONPs. The optimal batch (RA6) exhibited the smallest particle size, highest thermal stability, highest magnetization, and highest drug release rate. This suggests that a stirring speed of 900 RPM is ideal for producing IONPs with optimal properties. Higher RPM likely ensures uniform mixing and prevents particle aggregation, leading to smaller and more stable nanoparticles. The comparison between all reaction parameters (extract proportion, time, temperature, pH, and RPM) and the obtained evaluation characteristics is illustrated in the Figure 16-21.

CONCLUSION

The use of *Pimenta dioica* extract in the green synthesis of iron oxide nanoparticles (IONPs) is governed by various process parameters, each significantly impacting the resulting properties of the nanoparticles. The optimal conditions for synthesizing IONPs with desirable characteristics were identified as:

Extract proportion: 2:1 (AE2)

Synthesis time: 2-3 hours (TA2, TA3)

Temperature: 60-80°C (TEA3-TEA5)

pH: 10-11 (PA3, PA4)

RPM: 900 (RA6)

Under these conditions, the synthesized IONPs exhibited small particle sizes, high thermal stability, enhanced magnetization, and effective drug release rates, which are crucial for pharmaceutical applications. The study demonstrates the potential of *Pimenta dioica* extract as an efficient reducing and stabilizing agent for green synthesis of IONPs.

However, further specification and optimization are needed through factorial design experiments, where different combinations of the above-mentioned parameters can be interchanged to identify the most influential factors and their interactions. This approach will enable a more comprehensive understanding of the relationships between the process parameters and nanoparticle characteristics.

Acknowledgements

We gratefully acknowledge the Department of Chemistry at Dr. D. Y. Patil College of Pharmacy, Akurdi Pune, for their invaluable support and resources provided during the course of this research.

REFERENCES

1. Suci M, Ionescu CM, Ciorita A, Tripon SC, Nica D, Al-Salami H, Barbu-Tudoran L. Applications of superparamagnetic iron oxide nanoparticles in drug and therapeutic delivery, and biotechnological

- advancements. *Beilstein Journal of Nanotechnology*. 2020;11:1092–1109.
- Mondal P, Anweshan A, Purkait MK. Green synthesis and environmental application of iron-based nanomaterials and nanocomposite: A review. *Chemosphere*. 2020; 1; 259-127509 DOI: 10.1016/j.chemosphere.2020.127509
 - Xie J, Chen K, Huang J, Lee S, Wang J, Gao J, Li X, Chen X. PET/NIRF/MRI triple functional iron oxide nanoparticles. *Biomaterials*. 2010; 31(11): 3016-3022. DOI: 10.1016/j.biomaterials.2010.01.010
 - Paramasivam, D, Vadivel A, Chinnaperumal K, Govindasamy B, Dilipkumar A, Pachiappan P. Chemical and green synthesis of nanoparticles and their efficacy on cancer cells. In *Green synthesis, characterization and applications of nanoparticles*. Elsevier. 2019; 1: 369-387.
 - Pal G, Rai P, Pandey A. Green synthesis of nanoparticles: A greener approach for a cleaner future. *Elsevier*. 2019; 1: 1-26.
 - Rao PS, Navinchandra S, Jayaveera KN. An important spice, *Pimenta dioica* (Linn.) Merrill: A review. *International Current Pharmaceutical Journal*. 2012; 5;1(8):221-225. DOI:10.3329/icpj.v1i8.11255
 - Mahaparale SP, Patil AR. Ferric and Ferrous Molar Ratio Effect on Physical and Magnetic Properties of Iron Oxide Nanoparticles. *Iranian Journal of Materials Science & Engineering*. 2024; 21(1): 1-8.
 - Vongsak B, Sithisarn P, Mangmool S, Thongpraditchote S, Wongkrajang Y, Gritsanapan W. Maximizing total phenolics, total flavonoids contents and antioxidant activity of *Moringa oleifera* leaf extract by the appropriate extraction method. *Industrial crops and products*. 2013; 44: 566-571. DOI:10.1016/j.indcrop.2012.09.021
 - Milenković A, Stanojević J, Stojanović RZ, Pejić M, Cvetković D, Zvezdanović J, Stanojević L. Chemical composition, antioxidative and antimicrobial activity of allspice (*Pimenta dioica* (L.) Merr.) essential oil and extract. *Advanced Technologies*. 2020; 9(1):27-36. DOI:10.5937/savteh2001027M
 - Besenhard MO, LaGrow AP, Hodzic A, Kriechbaum M, Panariello L, Bais G, Loizou K, Damilos S, Cruz MM, Thanh NT, Gavriilidis A. Co-precipitation synthesis of stable iron oxide nanoparticles with NaOH: New insights and continuous production via flow chemistry. *Chemical Engineering Journal*. 2020; 1: 399-125740. DOI: 10.1016/j.cej.2020.125740.
 - Vitta Y, Figueroa M, Calderon M, Ciangherotti C. Synthesis of iron nanoparticles from aqueous extract of *Eucalyptus robusta* Sm and evaluation of antioxidant and antimicrobial activity. *Materials science for energy technologies*. 2020; 3: 97-103.
 - Karade VC, Dongale TD, Sahoo SC, Kollu P, Chougale AD, Patil PS, Patil PB. Effect of reaction time on structural and magnetic properties of green-synthesized magnetic nanoparticles. *Journal of Physics and Chemistry of Solids*. 2018; 120: 161-166. DOI:10.1016/j.jpcc.2018.04.040
 - Ozel F, Kockar H, Karaagac O. Growth of iron oxide nanoparticles by hydrothermal process: effect of reaction parameters on the nanoparticle size. *Journal of Superconductivity and Novel Magnetism*. 2015; 28: 823-829.
 - Park Y, Whitaker RD, Nap RJ, Paulsen JL, Mathiyazhagan V, Doerrer LH, Song YQ, Hürlimann MD, Szleifer I, Wong JY. Stability of superparamagnetic iron oxide nanoparticles at different pH values: experimental and theoretical analysis. *Langmuir*. 2012; 28(15): 6246-6255. DOI: 10.1021/la204628c
 - Ketebu O, Rhoda G, Oyinkepreye O. The Effect Of Revolution Per Minute (Rpm) On Iron Oxide Nanoparticles (Fe₃O₄Nps) Synthesis Through Direct Oxidative Alkaline Hydrolysis. *International Journal of Academic Research and Reflection*. 2015; 3(5): 90-98.
 - Laurent S, Bridot JL, Vander Elst L, Muller RN. Magnetic iron oxide nanoparticles for biomedical applications. *Future medicinal chemistry*. 2010; 2(3):427-449.
 - Laurent S, Forge D, Port M, Roch A, Robic C, Vander Elst L, Muller RN. Magnetic iron oxide nanoparticles: synthesis, stabilization, vectorization, physicochemical characterizations, and biological applications. *Chemical reviews*. 2008; 108(6): 2064-2610. <https://doi.org/10.1021/cr068445e>
 - Woo K, Hong J, Choi S, Lee HW, Ahn JP, Kim CS, Lee SW. Easy synthesis and magnetic properties of iron oxide nanoparticles. *Chemistry of materials*. 2004; 16(14): 2814-2818.
 - Cahyono B, A'yun Q, Suzery M. Characteristics of eugenol loaded chitosan-tripolyphosphate particles as affected by initial content of eugenol and their in-vitro release characteristic. In *IOP Conference Series: Materials Science and Engineering*. 2018; 349 (1), 012010; IOP Publishing. DOI:10.1088/1757-899X/349/1/012010
 - Nosrati H, Sefidi N, Sharafi A, Danafar H, Manjili HK. Bovine Serum Albumin (BSA) coated iron oxide magnetic nanoparticles as biocompatible carriers for curcumin-anticancer drug. *Bioorganic chemistry*. 2018; 1(76): 501-509.
 - Chawla A, Devhare LD, Dharmamoorthy G, Ritika, Tyagi S. Synthesis and In-vivo Anticancer Evaluation of N-(4-oxo-2-(4-((5-aryl-1,3,4 thiadiazole-2yl) amino) Phenyl thiazolidine-3-yl) Benzamide derivative. *International Journal of Pharmaceutical Quality Assurance*. 2023; 14(3):470-474.
 - Gnana RPM, Devhare LD, Dharmamoorthy G, Khairnar MV, Prasadha R. Synthesis, Characterisation, Molecular Docking Studies and Biological Evaluation of Novel Benzothiazole Derivatives as EGFR Inhibitors for Anti-breast Cancer Agents. *International Journal of Pharmaceutical Quality Assurance*. 2023; 14(3):475-480. DOI:10.25258/ijpqa.14.3.03
 - Choudhary RK, Beeraka S, Sarkar BK, Dharmamoorthy G, Devhare L. Optimizing Verapamil Hydrochloride In-situ Delivery: A Strategic Formulation Approach using Box-Behnken Design for Enhanced Performance and Comprehensive Evaluation of Formulation Parameters.

- International Journal of Drug Delivery Technology. 2024;14(1):61-70.
24. Kumar KK, Kiran V, Choudhary RK, Devhare LD, Gunjal SD. Design Development and Characterization of Nicardipine Solid Lipid Nano-Particulars. International Journal of Drug Delivery Technology. 2024; 14(1):71-78. DOI:10.25258/ijddt.14.1.12
25. Priya MGR, Prasanth LML, Devhare LD, Yazdan SK, Gunjal S. Synthesis, DNA Binding, Molecular Docking and Anticancer Studies of Copper (II), Nickel (II), and Zinc (II) Complexes of Primaquine-based Ligand. International Journal of Pharmaceutical Quality Assurance. 2024; 15(1):69-75. DOI:10.25258/ijpqa.15.1.10.